View Article Online / Journal Homepage / Table of Contents for this issue
Dynamic Article Links

Lab on a Chip

Cite this: *Lab Chip*, 2012, **12**, 4107–4114

www.rsc.org/loc

PAPER

Dual-channel bipolar electrode focusing: simultaneous separation and enrichment of both anions and cations†

Kyle N. Knust, Eoin Sheridan,‡ Robbyn K. Anand§ and Richard M. Crooks*

Received 12th June 2012, Accepted 9th August 2012
DOI: 10.1039/c2lc40660h

Downloaded by University of Texas Libraries on 20 December 2012
Published on 05 September 2012 on http://pubs.rsc.org | doi:10.1039/C2LC40660H

In this paper we show that a microelectrochemical cell comprising two parallel microchannels spanned by a single bipolar electrode can be used to simultaneously enrich and separate both anions and cations within a single microchannel. This is possible because reduction and oxidation of water at the cathodic and anodic poles of the bipolar electrode, respectively, lead to ion depletion zones. Specifically, $TrisH^+$ is neutralized by OH^- at the cathodic pole, while acetate buffer is neutralized by H^+ at the anodic pole. This action creates a local electric field gradient having both positive and negative components, and hence positive and negative ions follow their respective field gradients leading to separation. In the presence of an opposing counter-flow (pressure driven flow in this case), enrichment also occurs. In addition to separation and enrichment in a single channel, it is also possible to simultaneously enrich cations in one microchannel and anions in the other. Enrichment is achieved by controlling experimental parameters, including the type of buffer and the direction and magnitude of the opposing counter-flow.

Introduction

Detection of analytes within microfluidic devices often requires a preconcentration step prior to analysis. This is a consequence of small solution volumes, low concentrations, and hence small absolute numbers of molecules. We recently introduced an electrochemical technique, bipolar electrode (BPE) focusing, to address this issue.[1–7] BPE focusing is based upon balancing convective flow, which is nearly uniform in a noncompressible liquid, against electromigration (EM), which can be controlled locally along an electric field gradient. Here, we demonstrate that a dual-channel BPE focusing configuration can enrich and separate both anions and cations simultaneously. This is important, because a single platform may now be used for both cationic and anionic separation and enrichment.

We have previously shown that BPE focusing can separate and enrich anions in a single microchannel (Scheme 1).[1–7] In addition, our group has demonstrated the use of BPEs for depletion and membraneless filtration.[8] More recently, by adjusting the direction of electroosmotic flow (EOF), we have demonstrated enrichment of cations within a single-channel device.[9] Analogous to our single-channel studies, we have reported a dual-channel configuration (Scheme 2) that has some distinct advantages for enriching anions.[10] Here, we show that this same device configuration is a versatile platform for depletion, separation, and enrichment of charged analytes. The important new result is that it enables the simultaneous enrichment and separation of a mixture of anions and cations, which was previously unachievable in simple, single-channel fluidic devices.

BPE focusing is a member of a family of analyte enrichment techniques that is based on the principle of electrokinetic equilibrium. Methods in this family include counter-flow gradient focusing (CFGF),[11,12] isoelectric focusing (IEF),[13,14] field amplified sample stacking (FASS),[15,16] and isotachophoresis (ITP).[17,18] BPE focusing lies within the subfamily of CFGF methods, which also includes dynamic field gradient focusing (DFGF),[19,20] electric field gradient focusing (EFGF),[21,22] and temperature gradient focusing (TGF).[23,24] In all of these CFGF techniques, a local electric field is established within a fluidic channel, and used to control the electrophoretic velocity of a charged analyte. The electrophoretic force is then balanced against convective flow, and at the location where the forces sum to zero the analyte stops and enriches. The main difference between CFGF methods depends on how the local field is generated. In BPE focusing, it is produced electrochemically. Several of these electrokinetic equilibrium techniques have been used for the simultaneous separation and enrichment of analytes.[3,24–27] For example, Ivory *et al.* recently

Department of Chemistry and Biochemistry, Center for Electrochemistry, and the Center for Nano- and Molecular Science and Technology, The University of Texas at Austin, 1 University Station, A5300, Austin, Texas 78712-0165, USA. E-mail: crooks@cm.utexas.edu, Voice: 512-475-8674

† Electronic supplementary information (ESI) available: Enrichment experiments with $TrisH^+$ buffer in the bottom channel, representative measurements of the floating potential of the BPE, an explanation for the existence of both positive and negative electric fields in the bottom channel, evidence of simultaneous anion and cation separation and enrichment in the top channel, and movies of $Ru(bpy)_3^{2+}$ depleting from the bottom channel and $BODIPY^{2-}$ enriching on either side of the BPE anode. See DOI: 10.1039/c2lc40660h

‡ Present address: School of Mathematics and Physics, The University of Queensland, Brisbane, St Lucia, Queensland 4072, Australia
§ Present address: Department of Chemistry, University of Washington, Box 351700, Seattle, Washington 98195-1700, USA

Downloaded by University of Texas Libraries on 20 December 2012
Published on 05 September 2012 on http://pubs.rsc.org | doi:10.1039/C2LC40660H

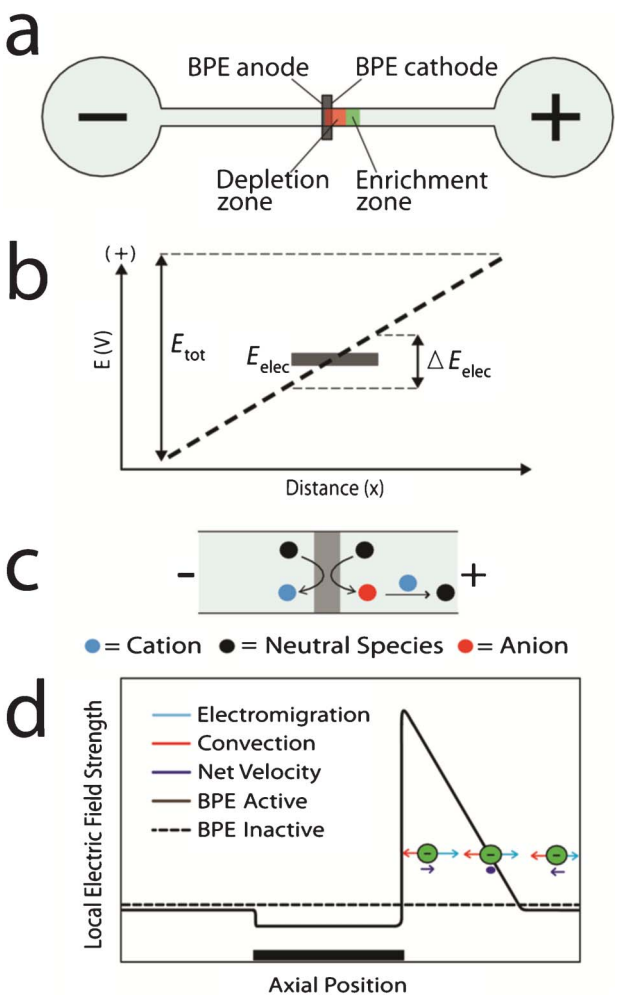

Scheme 1

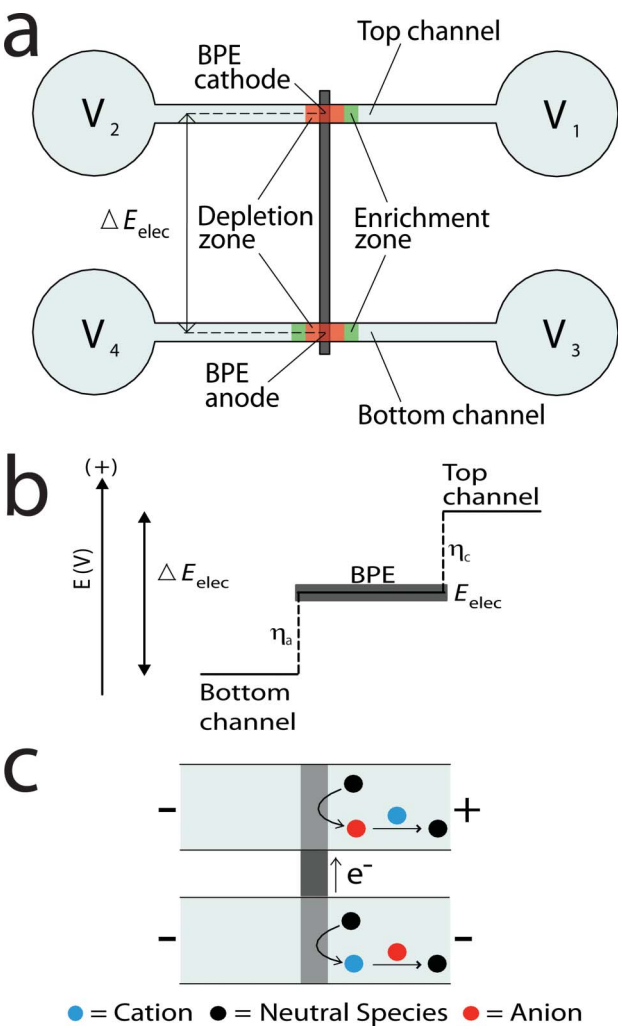

Scheme 2

reported an especially relevant example of DFGF which resulted in the separation and enrichment of cations and anions.[28] They accomplished this using a platform consisting of acrylic, ceramic, and membrane layers, along with a purge channel to remove electrolysis products. The effect was to produce a multi-component electric field with EM of charged analytes in multiple directions, which are requirements for simultaneously separating and enriching cations and anions. To the best of our knowledge, Ivory's DFGF is the only other reported example of simultaneous anion and cation separation and enrichment.

BPE focusing in the dual-channel configuration is analogous to another enrichment technique known as ion concentration polarization (ICP).[10] ICP produces an ion depletion zone when a potential bias applied across two compartments causes a large proportion of ionic current to be carried by either anions or cations through a perm-selective material such as Nafion or a nanochannel that exhibits overlap of the electrical double layer.[29,30]

The dual-channel device presented in Scheme 2 avoids complex fabrication methods, but still enables separation and enrichment of $BODIPY^{2-}$ and $Ru(bpy)_3^{2+}$ by more than 100-fold.[9,28] Electric field measurements reveal that faradaic reactions occurring at a BPE spanning two microfluidic channels generate two ion depletion and three enrichment zones. Specifically, $TrisH^+$ is neutralized by OH^- in the top channel, while in the bottom channel acetate buffer is neutralized by H^+. Under focusing conditions, the strength of the axial electric field was measured in discrete segments along both the top and bottom channels. These measurements demonstrate that stable enrichment is dependent upon the formation of an ion depletion zone and subsequent formation of an electric field gradient. In contrast to previous studies in which enrichment was limited to a region adjacent to one end of the BPE, tracer in the dual-channel scheme can enrich on either side of the BPE because the voltage drop creates unique mass transport conditions.[1–7,9] Electric field gradients in the bottom channel were also shown to contain multiple components which allow enrichment of $BODIPY^{2-}$, $Ru(bpy)_3^{2+}$, or both in a single microchannel.

Experimental section

Chemicals

The fluorescent tracers, 4,4-Difluoro-1,3,5,7,8-pentamethyl-4-bora-3a,4a-diaza-s-indacene-2,6-disulfonic acid ($BODIPY^{2-}$, Invitrogen, Carlsbad, CA) and 98% Tris (2,2′-bipyridyl) ruthenium(II) chloride

 This journal is © The Royal Society of Chemistry 2012

Downloaded by University of Texas Libraries on 20 December 2012
Published on 05 September 2012 on http://pubs.rsc.org | doi:10.1039/C2LC40660H

hexahydrate ($Ru(bpy)_3^{2+}$, Strem Chemicals, Newburyport, MA), were used for enrichment experiments. Poly(dimethylsiloxane) (PDMS) channels were prepared using a silicone elastomer and curing agent (Sylgard 184) from K.R. Anderson, Inc. (Morgan Hill, CA). A 0.5 M stock solution of Tris-$HClO_4$ (pH 8.1) was prepared from reagent grade Tris(hydroxymethyl)aminomethane (Sigma-Aldrich, St. Louis, MO) by dissolution in deionized water (18.0 MΩ cm, Milli-Q Gradient System, Millipore, Bedford, MA) and titration with 2.0 N $HClO_4$ (Ricca Chemical Co., Arlington, TX). This stock solution was then diluted to 40 mM (pH 8.1) and used as background electrolyte. A 0.5 M stock solution of acetate buffer (pH 4.8) was prepared from reagent grade sodium acetate (trihydrate, EMD Chemicals, Gibbstown, NJ) by dissolution in 18.0 MΩ cm deionized water (Millipore) and titration with 0.5 M HPLC-grade glacial acetic acid (Fisher Scientific, Fair Lawn, NJ). This stock solution was then diluted to 40 mM (pH 4.8) and used as background electrolyte.

Device fabrication

The procedure for assembling the PDMS/glass microfluidic devices has been previously published.[31] Briefly, 100 nm-thick and 250 μm-wide Au electrodes with no adhesion layer (Evaporated Metal Films, Ithaca, NY) were patterned on glass slides using AZ P4620 photoresist (AZ Electronic Materials, Somerville, NJ) and standard photolithographic techniques. These BPEs were fabricated with continuous and split poles.[4] Two PDMS microchannels (6.0 mm long, 50 μm wide, and 8.7 μm tall) were fabricated from a SU-8 5 (MicroChem, Newton, MA) mold patterned on a silicon wafer (University Wafer, South Boston, MA). The separation between the parallel channels was 9.0 mm (center-to-center). The PDMS channels were rinsed with ethanol and dried under N_2, then the PDMS and glass surfaces were exposed to an O_2 plasma (60 W, model PDC-32G, Harrick Scientific, Ossining, NY) for 15 s, and finally the two parts were bound together with the BPE aligned at the channel center. The PDMS/glass microfluidic device was then placed in an oven at 65 °C for 5 min to promote irreversible bonding.

Concentration enrichment experiments

Prior to each experiment, the microfluidic channels were rinsed using electroosmosis for 5 min with either 40 mM $TrisH^+$ buffer (pH 8.1) or 40 mM acetate buffer (pH 4.8) by applying 10.0 V to V_1 and V_3 while grounding V_2 and V_4 (Scheme 2a). Because EOF is somewhat suppressed at pH 4.8, pressure driven flow (PDF) was also used to rinse the channels.[32] Next, the rinse buffer was removed from the microchannels and replaced with 60.0 μL of 40 mM buffer containing 1.0 μM $BODIPY^{2-}$, 10.0 μM $Ru(bpy)_3^{2+}$, or a mixture of 1.0 μM $BODIPY^{2-}$ and 10.0 μM $Ru(bpy)_3^{2+}$.

Using a custom-built power supply incorporating a C-series voltage source (Ultra Volt, Ronkonkoma, NY), 30.0 V was applied to V_1, with V_2, V_3, and V_4 grounded. The driving electrodes were coiled Au wires immersed in each of the four reservoirs. Enrichment of fluorescent tracer was observed using an inverted epifluoresence microscope (Eclipse TE 2000-U, Nikon, Tokyo, Japan) fitted with a CCD camera (Cascade 512B, Photometrics, Tucson, AZ). PDF was initiated by creating a solution height differential in the reservoirs at the ends of the channel by adding or removing buffer. Measurements of PDF were estimated by tracking the movement of enriched bands after the 30.0 V driving potential was turned off, in which case all mass transport was due to PDF.

Images were collected and analyzed with image processing software (V++ Precision Digital Imaging, Auckland, New Zealand). A calibration of fluorescence intensities *vs.* concentration was used to determine the enrichment factor (EF) by dividing the maximum tracer concentration in the enriched band by the initial tracer concentration, with all measurements being corrected for background fluorescence intensity.

Electric field profile and voltage measurements

The axial electric field profile within the microchannels was monitored using a scanning digital multimeter (SDMM) (Model 2700, Keithley Instruments, Cleveland, OH) equipped with a multiplexer module (Model 7701, Keithley). The procedure for completing these measurements has been previously published.[6,7] The acquisition time for each voltage measurement was ~0.1 s, and the voltage between pairs of microbands recorded every 2.0 s. To collect the axial electric field profiles along the entire length of the 6.0 mm microchannel, eleven Au microbands (50 μm wide) were spaced 495 μm apart (center-to-center). As depicted in Fig. 1a and 1b, the centermost microband of these eleven was positioned between the split portion of the BPE. The two distal electric field measurements were made *vs.* the coiled Au electrodes placed in the reservoirs. Because of the manner the SDMM collects data, positive and negative electric fields were measured in the bottom channel. A similar finding was reported by Ivory and coworkers in their related simulations and experiments.[28,33] Additional details regarding these measurements is provided in the ESI.

The voltage dropped across both the top and bottom channels was obtained from the axial electric field measurements by adding together each voltage measurement made between microbands. The floating potential of the BPE, E_{elec}, was measured using a hand-held, digital multimeter equipped with PC-Link software (VA18B, Sinometer Instruments, Shenzhen, China). The potential difference between a microband extending from the BPE (Fig. 1a) and the driving electrode (V_1) was assigned to E_{elec}. Additional details regarding the measurement of E_{elec} can be found in the ESI.

Results and discussion

Basic principles of dual-channel enrichment

Most of our previous studies of BPE focusing have been directed toward BPEs embedded within a single microchannel (Scheme 1a).[1–9] If a sufficiently large voltage (E_{tot}) is applied across a buffer-filled microchannel containing a BPE, faradaic reactions, such as water oxidation and reduction, may occur at the poles of a BPE (Schemes 1b and 1c). These redox processes may lead to neutralization of the buffer, and in this case an ion depletion zone forms causing a sharp, local increase in solution resistance and hence an electric field gradient. Charged analytes then concentrate along this locally generated electric field gradient when convective flow is balanced against EM (Scheme 1d).

Downloaded by University of Texas Libraries on 20 December 2012
Published on 05 September 2012 on http://pubs.rsc.org | doi:10.1039/C2LC40660H

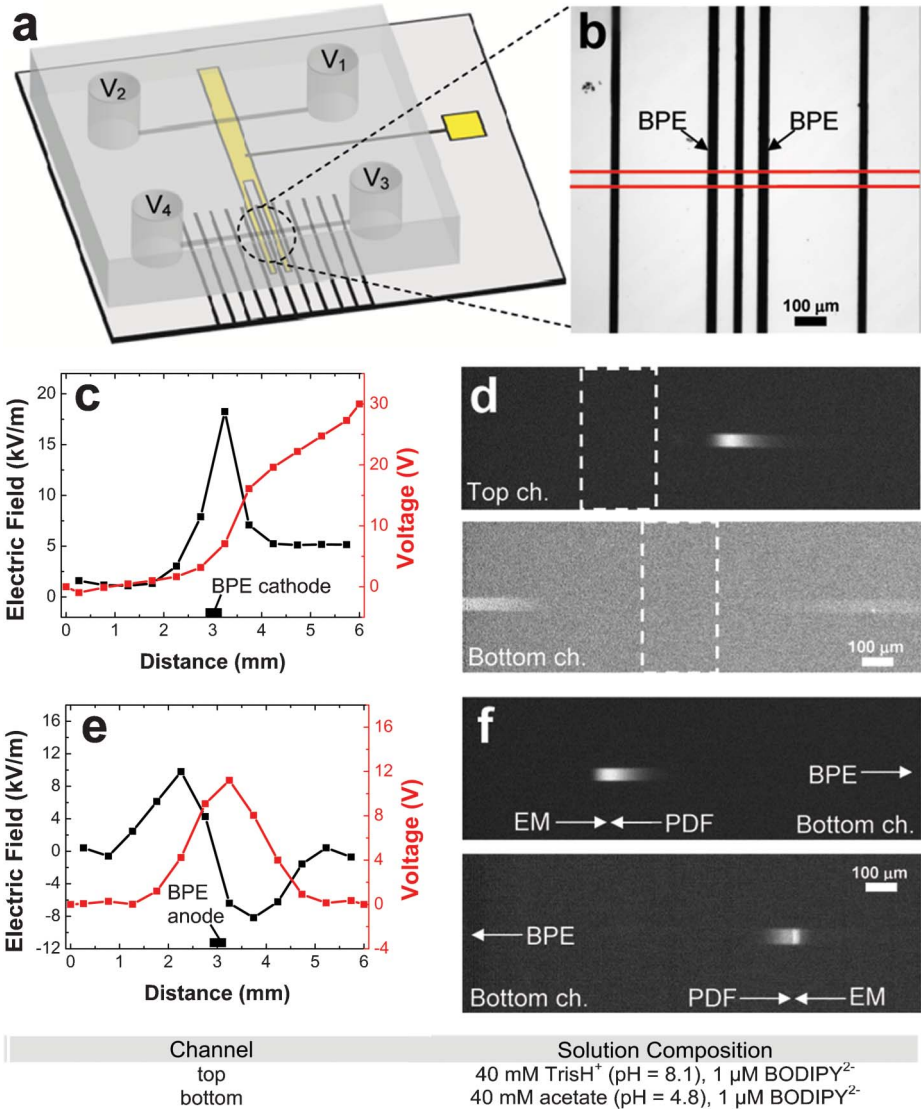

Fig. 1 (a) Graphic illustrating the device used to measure the axial electric field gradient. (b) Optical micrograph showing a close-up of a split BPE and flanking microband electrodes used to measure the electric field. (c) Plot of the axial electric field (black trace) and voltage drop (red trace) in the top channel. (d) Fluorescence micrographs of enriched $BODIPY^{2-}$ bands in the top and bottom channels with the location of the BPE indicated by dashed white lines. (e) Plot of the axial electric field (black trace) and voltage drop (red trace) in the bottom channel. (f) Fluorescence micrographs of enriched $BODIPY^{2-}$ bands in the bottom channel with PDF = $\sim$30 µm s^{-1} from right to left and left to right. The solution conditions are provided in the figure. V_1 = 30.0 V and V_2, V_3, and V_4 were grounded.

The basic operating principles of the dual-channel configuration (Scheme 2) are similar to those of the single-channel device. Specifically, ΔE_{elec}, which is the potential difference between the poles of the BPE, must exceed the redox potential for water oxidation and reduction (Scheme 2b).[5] If this condition is met, then water oxidation (eqn (1)) may proceed at the BPE anode (bottom channel) to generate H^+ and electrons. Once water oxidation occurs, to maintain charge neutrality within the BPE, electrons shuttle through the BPE to reduce water (eqn (2)) at the cathode (top channel) and generate OH^-. If an appropriately charged buffer capable of being neutralized by the products of water electrolysis is placed in either channel, an ion depletion zone, and thus an electric field gradient, should result. For example, in the top channel (Scheme 2c), $TrisH^+$ may be neutralized by OH^- (eqn (3)), and in the bottom channel acetate buffer may be neutralized by H^+ (eqn (4)). Upon neutralization, counter ions of the buffers are transported by a combination of convection and EM to the reservoirs where they charge pair with the products of water electrolysis.[2]

$$2H_2O - 4e^- \leftrightarrow O_2 + 4H^+ \quad (1)$$

$$2H_2O + 2e^- \leftrightarrow H_2 + 2OH^- \quad (2)$$

$$TrisH^+ + OH^- \leftrightarrow Tris + H_2O \quad (3)$$

$$CH_3CO_2^- + H^+ \leftrightarrow CH_3CO_2H \quad (4)$$

The important point is that buffer neutralization and the formation of an ion depletion zone results in an electric field gradient where charged analytes may be enriched when convective flow balances EM.

 This journal is © The Royal Society of Chemistry 2012

Downloaded by University of Texas Libraries on 20 December 2012
Published on 05 September 2012 on http://pubs.rsc.org | doi:10.1039/C2LC40660H

Dual-channel focusing and depletion with TrisH$^+$ buffer in the top channel and acetate buffer in the bottom channel

To correlate the shape of the ion depletion zone to the local electric field within each microchannel, the axial electric field was measured. Fig. 1a shows the device configuration used for these experiments, and Fig. 1b is an optical micrograph of the channel center. It shows two microbands, labeled BPE, that (when connected external to the channel) comprise the split BPE, and three additional microbands used for measuring the electric field. Note, we have previously shown that split and continuous BPEs are equivalent.[4] The microchannel, outlined in red, runs perpendicular to the microband electrodes. For all experiments discussed in this subsection, the top channel was filled with 40 mM TrisH$^+$ buffer (pH 8.1) containing 1.0 μM BODIPY^{2-}, and the bottom channel was filled with 40 mM acetate buffer (pH 4.8) containing either 1.0 μM BODIPY^{2-} or 10.0 μM Ru(bpy)$_3^{2+}$. All experiments were carried out with V_1 at 30.0 V, and V_2, V_3, and V_4 grounded (Fig. 1a).

Under these conditions, the potential difference between the solution and the BPE poles (ΔE_{elec}, Scheme 2b) is sufficiently large to drive water electrolysis at each end of the BPE. As depicted in the red trace of Fig. 1c, the 30.0 V potential difference between reservoirs V_1 and V_2 deviates from linearity as a result of water reduction and corresponding neutralization of TrisH$^+$ in the top channel (eqn (2) and (3), respectively). This leads to a decrease in the number of charge carriers and induces the ion depletion zone illustrated in Scheme 2a. That is, because the resistivity in this region is much higher than elsewhere in the channel, a disproportionate percentage of E_{tot} drops here (Fig. 1c, red trace from ~3–4 mm) and a corresponding electric field gradient forms (Fig. 1c, black trace). Analyte enriches along the electric field gradient, *via* the CFGF mechanism described earlier, wherein EOF (in this case) balances EM. Accordingly, an enriched band of the anionic tracer, BODIPY^{2-}, is observed in Fig. 1d (top image) with an EF of 264-fold (1.5-fold/s).

The BPE floats to an equilibrium potential, E_{elec}, that depends on the voltage difference applied across the top and bottom channels. Moreover, because the BPE is a conductor, E_{elec} is the same in both the top and bottom channel (Scheme 2b).[5] Because the reservoirs in the bottom channel are grounded, it follows that a potential difference exists between the BPE anode and the bottom reservoirs (Fig. 1e, red trace). Clearly, then, E_{elec} plays a key role in determining the degree of enrichment in both channels and hence is important to measure. The experimental approach for measuring E_{elec} is discussed in the ESI.

We now turn to processes occurring in the bottom channel. When filled with acetate buffer, a steep electric field gradient is observed as a result of electrogenerated H$^+$ neutralizing acetate buffer (eqn (1) and (4)) and the resulting formation of an ion depletion region and subsequent electric field gradient (Fig. 1e, black trace). The electrochemical and chemical processes that lead to this effect are illustrated in Scheme 2c. We also demonstrated that when the bottom channel is filled with TrisH$^+$ buffer, a steep electric field gradient capable of supporting a significant degree of enrichment does not form because TrisH$^+$ buffer may not be neutralized by H$^+$ generated at the BPE anode. These experiments are described in the ESI. The key point is that with TrisH$^+$ buffer present in the bottom channel, an ion depletion zone does not result, therefore preventing enrichment. However, with acetate buffer in the bottom channel, an ion depletion zone does form, which supports enrichment *via* the CFGF mechanism.

As shown in Fig. 1e (red trace), the voltage in the bottom channel is highest at the channel center and decreases to 0 V at each grounded reservoir. Interestingly, this causes BODIPY^{2-} to migrate toward the channel center, leading to tracer accumulation (Fig. 1d, bottom image) that is weak (51-fold, 0.3-fold/s) due to a lack of convective flow. There is no EOF in the bottom channel because the only possible direction for EOF would be from the channel center toward each of the grounded reservoirs. This would require the formation of a liquid-free zone, which is clearly not possible. It's also worth noting that there is no electric field directly above the BPE anode, and therefore BODIPY^{2-} does not accumulate there. However, if BODIPY^{2-} is replaced with cationic Ru(bpy)$_3^{2+}$ in the bottom channel, the direction of tracer EM reverses, thus resulting in Ru(bpy)$_3^{2+}$ depletion. There is a video of this process in the ESI.

Tracer enrichment is quite different when convection, in the form of PDF (~30 μm s^{-1}), is introduced in the bottom channel. In this case, a compact enriched band of BODIPY^{2-} forms (Fig. 1f, top image, EF = 357-fold, 1.0-fold/s). Enrichment occurs because PDF counters EM along the electric field gradient. If the PDF (~30 μm s^{-1}) is in the opposite direction, an enriched BODIPY^{2-} band is observed only on the opposite side of the BPE anode (Fig. 1f, bottom image, EF = 154-fold, 0.9-fold/s). A movie showing BODIPY^{2-} enrichment as a function of PDF direction is provided in the ESI.

The location of BODIPY^{2-} enrichment can be altered, because EM is in opposite directions on either side of the BPE anode. This behavior is not possible in a single-channel device because the direction of EM is uniform throughout the channel.[1–3] Moreover, single-channel devices produce a strong electric field gradient along only one edge of the BPE, similar to that observed in the top channel of the dual-channel device, Fig. 1c. However, with a multi-component electric field gradient in the bottom channel of the dual-channel scheme, the enrichment location may be determined by simply adjusting the direction of PDF.

With PDF in the bottom channel, the ion depletion regions shift, and hence the electric field gradients also change position.[7] Fig. 2a shows the electric field gradient with PDF (~30 μm s^{-1}) from right to left. During the course of this experiment, acetate electromigrates toward the channel center, while H$^+$ (produced at the BPE) electromigrates toward the channel reservoirs. This means that with PDF from right to left, the H$^+$ concentration in the 0 to 3 mm region of the microchannel increases, the neutralization reaction occurs to a greater extent, and therefore the slope of the electric field increases. Conversely, the electric field gradient in the 3 mm to 6 mm region is more shallow under these conditions. When the PDF is increased 4-fold, to ~120 μm s^{-1}, these effects are even more pronounced (Fig. 2b).

Fig. 2c shows that the location of Ru(bpy)$_3^{2+}$ enrichment can also be controlled by changing the direction of PDF (~90 μm s^{-1} in this case) in the bottom channel. Note, however, that for a particular direction of PDF, the enriched band of Ru(bpy)$_3^{2+}$ is on the opposite side of the BPE compared to that observed for BODIPY^{2-}. This is because EM is in opposite directions (within

Downloaded by University of Texas Libraries on 20 December 2012
Published on 05 September 2012 on http://pubs.rsc.org | doi:10.1039/C2LC40660H

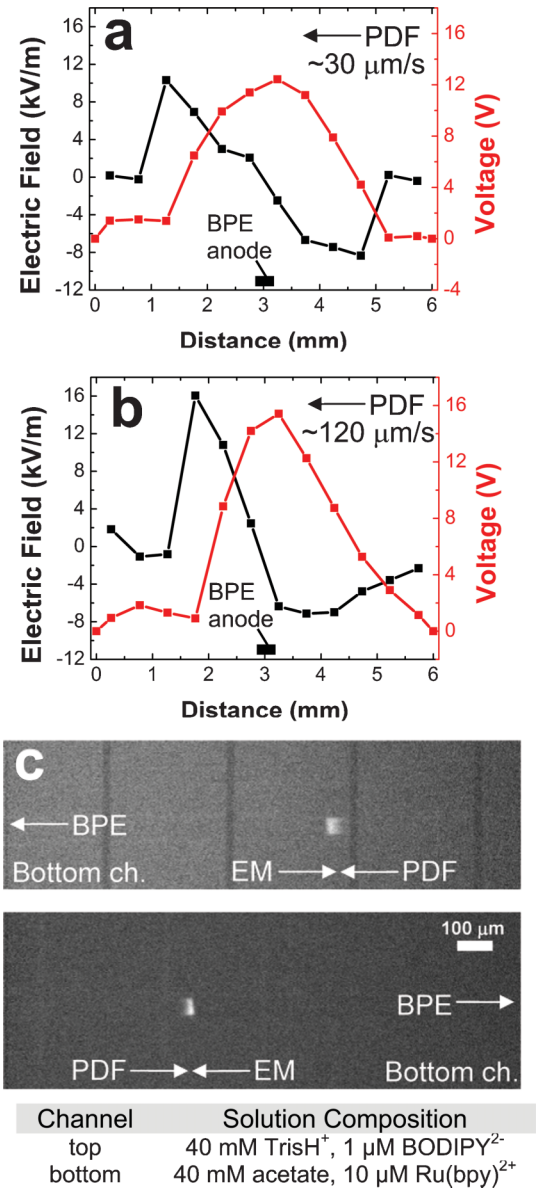

Fig. 2 Plot of the axial electric field (black trace) and voltage drop (red trace) in the bottom channel with PDF = ~30 μm s^{-1} (a) and PDF = ~120 μm s^{-1} (b) from right to left. (c) Fluorescence micrographs of enriched $Ru(bpy)_3^{2+}$ bands in the bottom channel with PDF = ~90 μm s^{-1} from right to left and left to right. The solution conditions are provided in the figure. V_1 = 30.0 V and V_2, V_3, and V_4 were grounded.

the same region of the microchannel) for tracers having opposite charges. Another interesting point is that the rate of enrichment for $Ru(bpy)_3^{2+}$ is lower than that of $BODIPY^{2-}$ (1-fold/s *vs.* 0.6-fold/s, respectively). This is because $Ru(bpy)_3^{2+}$ is transported by PDF from just one reservoir to the enrichment zone, while $BODIPY^{2-}$ is transported to the enrichment zone from both reservoirs by PDF and EM.

Simultaneous separation and enrichment of anions and cations

For all experiments within this subsection, the top channel was filled with 40 mM $TrisH^+$ buffer (pH 8.1) containing 1.0 μM $BODIPY^{2-}$, and the bottom channel was filled with 40 mM acetate buffer (pH 4.8) containing 1.0 μM $BODIPY^{2-}$ and 10.0 μM $Ru(bpy)_3^{2+}$. All experiments were carried out with V_1 at 30.0 V, and V_2, V_3, and V_4 grounded (Scheme 2a).

Thus far we have shown that the enrichment location of both $BODIPY^{2-}$ and $Ru(bpy)_3^{2+}$ can be controlled in the bottom channel, because the voltage profile leads to EM in opposite directions in each half of the microchannel. Accordingly, with the multi-component electric field gradient in the bottom channel, it should be possible to separate and enrich mixtures of oppositely charged analytes. Fig. 3a summarizes the situation. Here, PDF is directed from left to right, and the direction of EM depends on the charge on the tracer. At the channel center, where there is no electric field strength, ions experience no EM; therefore, their net velocity is dictated exclusively by convection. Moreover, because there is no EOF in the bottom channel, convection depends only on PDF. To the left of the BPE anode, anions move toward the channel center by both EM and PDF. In the same region, cations also

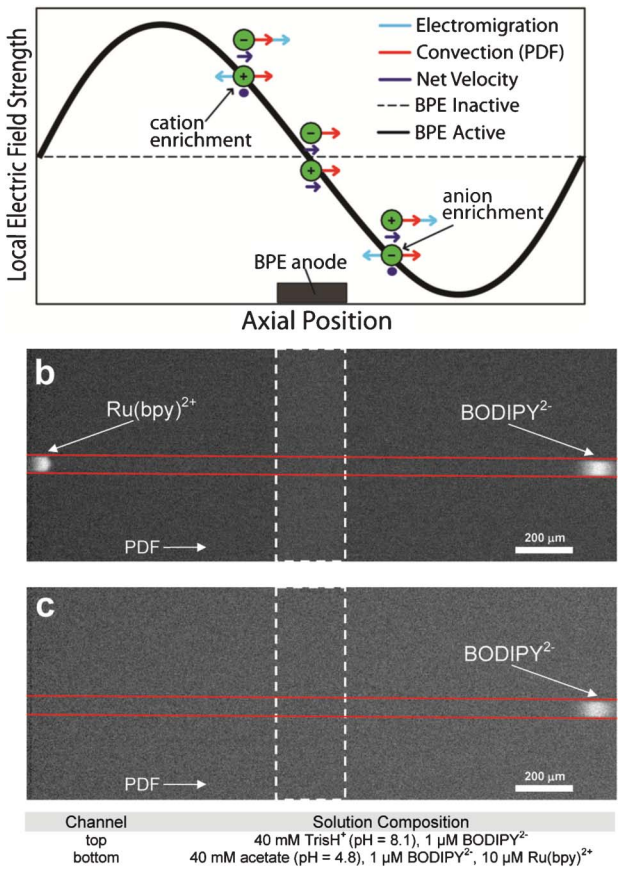

Fig. 3 (a) Schematic illustrating the direction of convection, EM, and net velocity of tracer in the bottom channel. (b) Fluorescence micrograph of enriched bands of $BODIPY^{2-}$ and $Ru(bpy)_3^{2+}$ in the bottom channel with PDF (~90 μm s^{-1}) from left to right. The location of the BPE is indicated by dashed white lines. (c) Fluorescence micrograph collected 3 s after Fig. 3b using a filter set capable of detecting only $BODIPY^{2-}$ showing an enriched $BODIPY^{2-}$ band only to the right of the BPE. The solution conditions are provided in the figure. V_1 = 30.0 V and V_2, V_3, and V_4 were grounded.

 This journal is © The Royal Society of Chemistry 2012

Downloaded by University of Texas Libraries on 20 December 2012
Published on 05 September 2012 on http://pubs.rsc.org | doi:10.1039/C2LC40660H

experience PDF toward the channel center, but EM is in the opposite direction so enrichment occurs. An analogous argument can be made on the right side of the BPE anode for anion enrichment. In principle, then, if the right magnitude of PDF (left to right) is chosen, cations will enrich to the left of the BPE anode and anions will enrich to its right.

In Fig. 3b, PDF ($\sim$90 μm s^{-1}) is directed from left to right. To the left of the BPE anode (indicated by dashed lines), $Ru(bpy)_3^{2+}$ (EF = 136-fold, 0.5-fold/s) enriches, while $BODIPY^{2-}$ (EF = 113-fold, 0.4-fold/s) enriches to its right. This fluorescence micrograph was collected using a filter set capable of detecting both $BODIPY^{2-}$ and $Ru(bpy)_3^{2+}$. Three seconds after Fig. 3b was collected, another fluorescence micrograph (Fig. 3c) was recorded using a filter set capable of detecting only $BODIPY^{2-}$. In this micrograph, $BODIPY^{2-}$ enrichment occurs only to the right of the BPE anode, thereby confirming the identity of the two enriched bands. The important point is that the dual-channel microfluidic configuration leads to the simultaneous separation and enrichment of both anions and cations.

Although the EF for $Ru(bpy)_3^{2+}$ is greater than that of $BODIPY^{2-}$, as the experiment progresses, $BODIPY^{2-}$ continually enriches while $Ru(bpy)_3^{2+}$ enrichment plateaus. This is because $BODIPY^{2-}$ is transported to the enrichment region by both PDF and EM, while $Ru(bpy)_3^{2+}$ is transported to its enrichment location only by PDF. With $BODIPY^{2-}$ enriching at a steeper electric field gradient than $Ru(bpy)_3^{2+}$, this result is also consistent with the previous discussion showing changes in the electric field gradient with respect to the magnitude of PDF.

In addition to simultaneously separating and enriching both anions and cations in the bottom channel, an analogous result may be achieved in the top channel by changing the voltage configuration. With V_1 and V_2 at 30.0 V and V_3 and V_4 grounded (Scheme 2a), the voltage drop and electric field gradient in the top channel are likely similar to that observed in the bottom channel with the difference being that voltage drops from the reservoirs toward the channel center where the ion depletion zone and region of high resistivity forms. As discussed in the ESI, qualitative evidence of this was observed when anions and cations were found to simultaneously separate and enrich in both the top and bottom channels with this new voltage configuration applied.

Summary and conclusions

The key finding reported in this paper is that the dual-channel BPE focusing scheme can be used to produce multiple ion depletion and enrichment zones. Moreover, the unique mass transport properties and multi-component electric field gradient that forms in the bottom channel provides a means to simultaneously separate and enrich anions and cations in a single microchannel. This result was previously unachievable in single-channel, BPE fluidic devices. The dual-channel microelectrochemical platform requires only simple fabrication procedures and facilitates enrichment of cations, anions, or both, all while controlling the enrichment location. Therefore, with the capability of enriching and transporting anions and cations on an inclusive platform, the analysis of complex mixtures of charged analytes may be realized.

Major symbols and abbreviations

BPE	bipolar electrode
CFGF	counter-flow gradient focusing
E_{elec}	floating potential of the bipolar electrode
ΔE_{elec}	potential difference between the poles of the bipolar electrode
EF	enrichment factor
EM	electromigration
EOF	electroosmotic flow
E_{tot}	applied voltage between driving electrodes
PDF	pressure driven flow

Acknowledgements

We gratefully acknowledge support from the Chemical Sciences, Geosciences, and Biosciences Division, Office of Basic Energy Sciences, Office of Science, U.S. Department of Energy (contract no. DE-FG02-06ER15758). The Robert A. Welch Foundation provides sustained support for our research (Grant F-0032).

References

1 R. Dhopeshwarkar, D. Hlushkou, M. Nguyen, U. Tallarek and R. M. Crooks, *J. Am. Chem. Soc.*, 2008, **130**, 10480–10481.
2 D. Hlushkou, R. K. Perdue, R. Dhopeshwarkar, R. M. Crooks and U. Tallarek, *Lab Chip*, 2009, **9**, 1903–1913.
3 D. R. Laws, D. Hlushkou, R. K. Perdue, U. Tallarek and R. M. Crooks, *Anal. Chem.*, 2009, **81**, 8923–8929.
4 R. K. Perdue, D. R. Laws, D. Hlushkou, U. Tallarek and R. M. Crooks, *Anal. Chem.*, 2009, **81**, 10149–10155.
5 F. Mavré, R. K. Anand, D. R. Laws, K.-F. Chow, B.-Y. Chang, J. A. Crooks and R. M. Crooks, *Anal. Chem.*, 2010, **82**, 8766–8774.
6 E. Sheridan, D. Hlushkou, R. K. Anand, D. R. Laws, U. Tallarek and R. M. Crooks, *Anal. Chem.*, 2011, **83**, 6746–6753.
7 R. K. Anand, E. Sheridan, D. Hlushkou, U. Tallarek and R. M. Crooks, *Lab Chip*, 2011, **11**, 518–527.
8 E. Sheridan, K. N. Knust and R. M. Crooks, *Analyst*, 2011, **136**, 4134–4137.
9 E. Sheridan, D. Hlushkou, K. N. Knust, U. Tallarek and R. M. Crooks, *Anal. Chem.*, 2012, DOI: 10.1021/ac301101b.
10 R. K. Anand, E. Sheridan, K. N. Knust and R. M. Crooks, *Anal. Chem.*, 2011, **83**, 2351–2358.
11 N. T. Tran, I. Ayed, A. Pallandre and M. Taverna, *Electrophoresis*, 2010, **31**, 147–173.
12 J. G. Shackman and D. Ross, *Electrophoresis*, 2007, **28**, 556–571.
13 H. Cui, K. Horiuchi, P. Dutta and C. F. Ivory, *Anal. Chem.*, 2005, **77**, 1303–1309.
14 D. Kohlheyer, J. C. T. Eijkel, S. Schlautmann, A. van den Berg and R. B. M. Schasfoort, *Anal. Chem.*, 2007, **79**, 8190–8198.
15 H. Yang and R. L. Chien, *J. Chromatogr., A*, 2001, **924**, 155–163.
16 B. Jung, R. Bharadwaj and J. G. Santiago, *Electrophoresis*, 2003, **24**, 3476–3483.
17 B. Jung, Y. Zhu and J. G. Santiago, *Anal. Chem.*, 2007, **79**, 345–349.
18 T. K. Khurana and J. G. Santiago, *Anal. Chem.*, 2008, **80**, 279–286.
19 Z. Huang and C. F. Ivory, *Anal. Chem.*, 1999, **71**, 1628–1632.
20 J. M. Burke, C. D. Smith and C. F. Ivory, *Electrophoresis*, 2010, **31**, 902–909.
21 P. H. Humble, R. T. Kelly, A. T. Woolley, H. D. Tolley and M. L. Lee, *Anal. Chem.*, 2004, **76**, 5641–5648.
22 R. T. Kelly and A. T. Woolley, *J. Sep. Sci.*, 2005, **28**, 1985–1993.
23 D. Ross and L. E. Locascio, *Anal. Chem.*, 2002, **74**, 2556–2564.
24 K. M. Balss, W. N. Vreeland, K. W. Phinney and D. Ross, *Anal. Chem.*, 2004, **76**, 7243–7249.
25 M. W. Kamande, D. Ross, L. E. Locascio, M. Lowry and I. M. Warner, *Anal. Chem.*, 2007, **79**, 1791–1796.
26 T. K. Khurana and J. G. Santiago, *Lab Chip*, 2009, **9**, 1377–1384.
27 D. W. Inglis, E. M. Goldys and N. P. Calander, *Angew. Chem., Int. Ed.*, 2011, **50**, 7546–7550.

View Article Online

28 J. M. Burke, Z. Huang and C. F. Ivory, *Anal. Chem.*, 2009, **81**, 8236–8243.
29 Y.-C. Wang, A. L. Stevens and J. Han, *Anal. Chem.*, 2005, **77**, 4293–4299.
30 S. J. Kim, Y.-A. Song and J. Han, *Chem. Soc. Rev.*, 2010, **39**, 912–922.
31 J. C. McDonald, D. C. Duffy, J. R. Anderson, D. T. Chiu, H. Wu, O. J. A. Schueller and G. M. Whitesides, *Electrophoresis*, 2000, **21**, 27–40.
32 G. Ocvirk, M. Munroe, T. Tang, R. Oleschuk, K. Westra and D. J. Harrison, *Electrophoresis*, 2000, **21**, 107–115.
33 J. M. Burke and C. F. Ivory, *Electrophoresis*, 2008, **29**, 1013–1025.

Downloaded by University of Texas Libraries on 20 December 2012
Published on 05 September 2012 on http://pubs.rsc.org | doi:10.1039/C2LC40660H

This journal is © The Royal Society of Chemistry 2012